fire

MDPI

Article

Study on Particulate Matter Emissions from Forest Combustible Material Combustion in the Xiao Xing'an Mountains Region with Random Forest and XGBoost Model Validation

Duaa Alshammari [1], Hui Huang [2], Haifeng Gao [3], Xiaoying Han [4], Mohammed Alsharam [5], Sarah Alathwari [6], Xiangxuan Zeng [7] and Zhan Shu [1,*]

[1] College of Forestry, Northeast Forestry University, No. 26 Hexing Road, Harbin 150040, China; duaa@nefu.edu.cn
[2] School of Water Conservancy and Civil Engineering, Heilongjiang Agricultural Engineering Vocational College, Harbin 150025, China; swkjhh@163.com
[3] Satellite Application Center for Ecology and Environment, Ministry of Ecology and Environment, Beijing 100006, China; gaohf03@hotmail.com
[4] Institute of Atmospheric Environment and Climate Change, Heilongjiang Academy of Environmental Sciences, Harbin 150000, China; 18646250280@163.com
[5] Software College, Northeastern University, Shenyang 110169, China; alsharam@stumail.neu.edu.cn
[6] College of Economics and Management, Northeast Forestry University, Harbin 150040, China; sarah@nefu.edu.cn
[7] Department of International Economics and Trade, Cheongju University, Cheongju 28503, Republic of Korea; zengxiangxuan@kakao.com
* Correspondence: shuzhan@nefu.edu.cn; Tel.: +86-451-82192030; Fax: +86-451-82192030

Abstract

This study tested whether fine particulate matter ($PM_{2.5}$) emissions from forest fuel combustion in the Xiao Xing'an Mountains are controlled by common or vegetation-category-specific factors. Six conifer, nine broad-leaved and seven shrub species were burned in a laboratory chamber (6966 measurements). Because the factors tested differed among categories, effects were analyzed within each category and compared across categories only for shared factors, using ANOVA, multiple linear regression, Random Forest and XGBoost. Fuel load was a primary factor in all three categories. In addition, $PM_{2.5}$ was controlled by moisture content, plant part and combustion mode in shrubs; by plant part, season and species in broad-leaved species; and by plant part and wind speed in conifers. Among the shared factors, moisture content had a clear effect only in shrubs (partial $\eta^2 = 0.16$ vs. ≤ 0.03 in trees). Smoldering tests produced 34% more $PM_{2.5}$ than flaming tests in shrubs ($p < 0.001$), and broad-leaved bark and branches had 89% higher $PM_{2.5}$ concentrations in April than in July. The mean shrub emission factor was 12.5 g/kg, without significant inter-species variation ($p = 0.668$). Under grouped five-fold cross-validation, Random Forest and XGBoost reached R^2 of 0.77–0.96, compared with 0.21–0.74 for linear models. The results support vegetation category as a stratification variable in regional forest-fire emission inventories.

Keywords: $PM_{2.5}$; forest fuel; emission factors; biomass burning; machine learning

Check for updates

Academic Editor: Long Yan

Received: 17 September 2026
Revised: 20 October 2026
Accepted: 3 November 2026
Published: 6 November 2026

Copyright: © 2026 by the authors. Licensee MDPI, Basel, Switzerland. This article is an open access article distributed under the terms and conditions of the Creative Commons Attribution (CC BY) license.

1. Introduction

Forest fires release substantial quantities of fine particulate matter with aerodynamic diameter ≤ 2.5 μm ($PM_{2.5}$) into the atmosphere, with well-documented consequences for air quality, human health, and climate forcing [1,2]. $PM_{2.5}$ from biomass combustion has

been linked to elevated cardiovascular and respiratory mortality, with fire smoke estimated to contribute significantly to carbonaceous $PM_{2.5}$ concentrations across large regions of the Northern Hemisphere [3,4]. The carbonaceous aerosol fraction influences radiation balance through both direct absorption (black carbon) and scattering (organic aerosols), making wildfire $PM_{2.5}$ a dual agent in the climate system [5,6]. As wildfire frequency, severity, and burned area continue to increase globally under climate change [7,8], the IPCC has identified biomass-burning aerosols—of which $PM_{2.5}$ is the dominant health-relevant component—as exerting short-lived but climatically significant radiative effects [9], underscoring the need for accurate, regionally specific characterization of $PM_{2.5}$ emissions from forest fuels.

In China, forest fires and open biomass burning are important sources of air pollution, and northeastern temperate forests are particularly vulnerable to wildfire [10,11]. Biomass burning—encompassing wildfires, prescribed burns, and agricultural residue combustion—is a dominant contributor to ambient $PM_{2.5}$ concentrations in the region, particularly during the spring fire season and winter heating period, when stable atmospheric conditions favor pollution accumulation [12–15]. Large-scale spatial analyses have demonstrated significant correlations between biomass burning intensity and $PM_{2.5}$ levels across China, with spatial heterogeneity driven by differences in vegetation composition, combustion conditions, and socioeconomic factors [16]. High-resolution emission inventories developed for Heilongjiang Province have highlighted persistent uncertainties from the limited availability of species-specific emission factors for the region's mixed coniferous-broad-leaved fuel types [2,17], and recent inventories have consistently identified forest and crop-residue burning as leading non-point $PM_{2.5}$ contributors during the spring fire window [16–18], yet a systematic, controlled assessment of how the dominant emission drivers vary among co-occurring conifers, broadleaf, and shrub fuels remains unavailable for the Xiao Xing'an Mountains.

Emission characteristics are governed by a complex interplay of fuel factors. Higher moisture content inhibits full oxidation and favors smoldering, a low-temperature, oxygen-limited mode that yields disproportionately high concentrations of organic aerosol and fine particles [19,20], and the significance of moisture in fire hazard and emission profiles is further highlighted by algorithms for calculating fuel moisture and fire maturation time [19]. The volatile fraction available for particle formation is determined by fuel type, plant part and chemical composition. Resinous conifer needles, cellulose-rich broadleaves and dense woody tissues have fundamentally different pyrolysis pathways and emission signatures [21–24]. This divergence is in agreement with the different thermal decomposition behavior of hemicellulose, cellulose, and lignin, which are the structural components controlling the characteristics of biomass pyrolysis and combustion pollutants [25,26]. The modified combustion efficiency also shows significant differences among vegetation types [22,27]. These differences affect the elemental versus organic carbon composition of the released $PM_{2.5}$ particles, with smoldering being characterized by mostly organic materials, and flaming by mostly elemental carbon [28,29]. This pattern changes throughout one burn, beginning from ignition and progressing towards steady flaming and smoldering [28]. The wind speed determines the oxygen level, flame shape, and burning rate, and thus it is included in many emission factor listings for smoke management.

Much of what is known about these controls comes from laboratory combustion of wildland fuels, in which fuel properties and burning conditions can be controlled. Large laboratory programs have measured $PM_{2.5}$ and trace-gas emission factors for many fuels from North America, Africa and Asia [22,30–33]. Their results, together with field data, have been compiled into emission-factor databases used by inventories and atmospheric models [27,34,35]. These compilations report $PM_{2.5}$ emission factors by broad biome or

fuel type, and the temperate mixed forests of northeastern Asia remain poorly represented. Machine-learning methods have recently been applied to $PM_{2.5}$ from forest-fuel combustion in northeastern China, with LightGBM, Random Forest and gradient boosting models for broad-leaved trees [36], conifers [37] and shrubs [38], respectively. Each of these studies treated a single vegetation category, so whether the controlling factors are shared among co-occurring vegetation categories has not been tested within one analytical framework.

The vegetation of the Xiao Xing'an Mountains area within Heilongjiang Province comprises coniferous, deciduous, and mixed forests, totaling over 78% of the area [39,40]. The dominant trees in the canopy layer include conifers such as *Pinus koraiensis* and *Larix gmelinii* together with deciduous trees such as *Acer* spp., *Ulmus* spp., and *Tilia* spp. The shrub layer includes *Corylus mandshurica* and *Acanthopanax senticosus*, which have high amounts of biomass above the ground [41–43]. Additive biomass models for the four major shrub species quantify the carbon pool available for rapid combustion [44], flammability testing has covered 12 regional shrub species [43], and further work has characterized forest fuel parameters and stand structure [39].

This vegetation diversity sits alongside a climate of dry springs and recurring fire [45,46], together making the Xiao Xing'an Mountains an ecologically important test case for $PM_{2.5}$ emission research. Historical fire records document frequent disturbance cycles, with considerable carbon stocks released over past decades [47]. Related regional work has quantified fire emissions in the Daxing'an Mountains [48], $PM_{2.5}$ from combustion at Liangshui National Natural Reserve [38,49], carbon-gas emissions from major Heilongjiang arbor species [24], the spatiotemporal pattern of forest-fire pollutant emissions across China [2,18], and fire-driven net primary productivity losses [50]. However, despite this body of work, no study has systematically compared $PM_{2.5}$ emissions across conifers, broad-leaved species, and shrubs from the same region under controlled conditions, or identified whether the dominant emission-controlling factors are consistent across vegetation categories or fundamentally category-specific.

This study addresses that gap through a laboratory-based experimental combustion study. Compared with previous laboratory studies that treated vegetation types in isolation, the key novelty of this work is a systematic, side-by-side comparison of the dominant controlling factors of $PM_{2.5}$ emissions among the three major vegetation categories of the Xiao Xing'an Mountains, analyzed with identical statistical and machine-learning procedures. To account for extraneous variables such as location, equipment, or seasonality, ignition conditions and chamber airflow were standardized within each experimental series, and replicated trials across 22 species provide a factorial dataset with greater statistical power than field data alone for detecting the main effects and interactions. Our central hypothesis holds that the key variables governing $PM_{2.5}$ emissions differ among vegetation categories, so that no single emission factor can adequately describe mixed forests. This study therefore pursues four goals: (1) quantifying $PM_{2.5}$ emissions during burning of leaves, branches, and bark across 22 species spanning conifers, broad-leaved species, and shrubs; (2) identifying the most critical environmental and fuel variables controlling $PM_{2.5}$ emissions in each category; (3) evaluating shrub species emission factors and their interspecies variability; and (4) developing category-specific statistical and machine-learning models for predicting $PM_{2.5}$ emissions.

2. Materials and Methods

2.1. Study Area

The Xiao Xing'an Mountains are situated in northeastern China, in the northern part of Heilongjiang Province, forming a northwest–southeast-trending mountainous forest region of approximately 90,000 km^2 (Figure 1), lying approximately between 126° E–132° E and 46°

N–50° N. Major cities within or near the mapped area include Heihe to the north, Yichun near the central forested area, and Hegang and Jiamusi to the southeast [40,51].

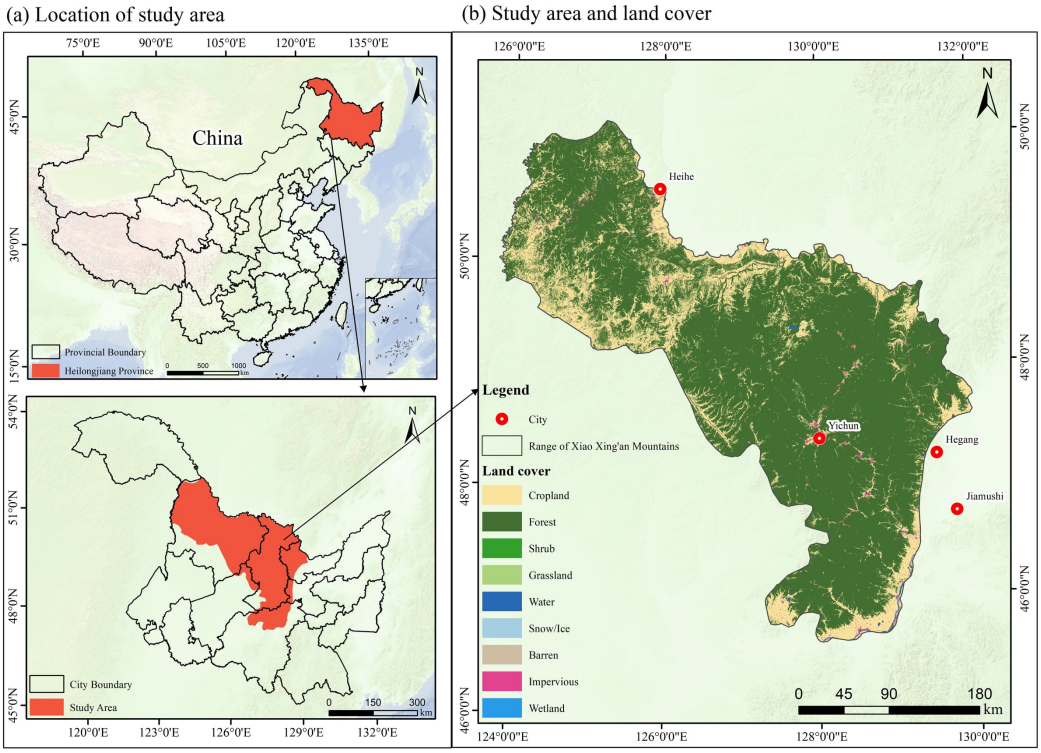

Figure 1. Location of the Xiao Xing'an Mountains study area and its land-cover pattern in Heilongjiang Province, northeastern China. Panel (**a**) shows the position of the study area within China and Heilongjiang Province; panel (**b**) shows the study-area boundary, major cities, and dominant land-cover classes, including cropland, forest, shrub, grassland, water, snow/ice, barren land, impervious surface, and wetland. The legend follows the full classification of the dataset; several classes occupy very small, scattered patches and are barely visible at this map scale. Note: map lines delineate study areas and do not necessarily depict accepted national boundaries. Land cover data are from the 30 m annual China Land Cover dataset [52].

Forest is the dominant cover type, forming a continuous belt through the central and southern range, with cropland concentrated along valleys and settlement margins and water bodies clustered toward the east and southeast; shrub, grassland, wetland, barren land, and impervious surfaces occupy smaller, scattered areas (Figure 1b). This reflects the region's temperate mixed coniferous-broadleaf forest: representative overstory species include *Pinus koraiensis*, *Larix gmelinii*, *Pinus sylvestris* var. mongolica, *Abies nephrolepis*, and *Picea* species, alongside broadleaf taxa such as *Acer* spp., *Tilia amurensis*, *Phellodendron amurense*, and *Ulmus* spp., with an understory shrub layer dominated by *Corylus mandshurica*, *Acanthopanax senticosus*, and *Syringa reticulata* var. *amurensis* [43,44].

The regional climate is temperate continental monsoon, with mean annual temperature of −1 to 1 °C, annual precipitation of 500–700 mm falling mostly in summer, and a frost-free period of 100–120 days [53,54], corroborated by direct meteorological tower observations of canopy-level CO_2 flux in the region [55]. Recurrent forest fires occur mainly during the dry spring (March–May) and autumn (September–November), when low humidity and accumulated surface fuels raise fire risk [45,47,56].

2.2. Experimental Design

Twenty-two species were selected to represent the three dominant vegetation categories of the Xiao Xing'an Mountains (Table S1): six conifer species, nine broad-leaved species,

and seven shrub species. The selection was based on ecological dominance and relevance to regional fire dynamics [39,43].

The three vegetation categories were originally studied in separate experimental series, and the factors varied were chosen to represent the conditions most relevant to each fuel type (Table 1). Wind speed was varied only for conifers, season only for broad-leaved species and combustion mode only for shrubs. The design is therefore fully crossed within each category but not across categories. The effects of the category-specific factors can be estimated only within their own category, and cross-category comparisons were restricted to the factors common to all three categories (species, plant part, moisture content and fuel load; Section 3.7). All conditions were measured in triplicate.

Table 1. Experimental design by vegetation category.

Category	Parts	MC (%)	Fuel Load (g)	Wind (m/s)	Combustion Mode	Season	$PM_{2.5}$ Unit
Conifers	Leaf, branch, bark	0, 5, 10, 15	0.5, 1, 2	0, 1, 2, 3	–	July	g per test
Broad-leaved	Leaf, branch, bark	0, 5, 10, 15, 20	1, 2, 3	–	–	Apr, Jul, Oct [a]	$\mu g\ m^{-3}$
Shrub	Leaf, branch	10, 15, 20, 25, 40 [b]	1, 2, 3	–	Flaming, smoldering	July	g per test

[a] In April, only branches and bark were sampled; broad-leaved species had not yet flushed at the budding stage, giving 8 season × part combinations rather than 9. [b] At 40% moisture content, flaming combustion could not be sustained; only smoldering tests were made, giving 1134 shrub measurements rather than 1260.

2.3. Sample Collection

In 2023, fuel samples were collected from representative forest stands in the Xiao Xing'an Mountains in collaboration with local forestry bureaus and the Liangshui National Nature Reserve [49]. Samples of broad-leaved species were taken in April, July and October to cover the whole phenological cycle; conifer and shrub samples were only taken in July. For each species, leaves, branches and bark were sampled from at least three individual plants per stand, transported to the laboratory in sealed containers and brought to the target moisture content either by oven-drying (40 °C) or by rewetting through equilibration with deionized water (≥12 h). The moisture content was determined gravimetrically to within ±1% prior to each combustion test. Branch samples were cut into 3–5 cm segments and all samples were weighed to ±0.0001 g.

The broad-leaved, conifer and shrub datasets were analyzed separately in earlier studies from our laboratory [36–38]. Here, the three datasets are integrated and re-analyzed with identical statistical and machine-learning procedures in order to compare their controlling factors.

2.4. Combustion Experiments

Laboratory combustion studies were performed using a chamber with $PM_{2.5}$ analysis equipment and a ventilation system, which allowed standardized ignition and ventilation to be monitored during each experiment. For coniferous samples, wind speed was set at four levels (0, 1, 2 and 3 m/s) using calibrated wind-blowing equipment set at a constant distance from the chamber inlet. Sampling duration was adjusted according to fuel type and moisture content to ensure complete capture of combustion emissions. Broad-leaved samples, which required longer burn times at higher moisture contents, were sampled for 26 min at 100 $L \cdot min^{-1}$ (0.1 $m^3 \cdot min^{-1}$), giving a sampled volume of 2.6 m^3 per measurement. Conifer

and shrub samples, which burned more rapidly, required shorter sampling durations (17 min for shrubs). Levels were chosen to reproduce environmental conditions associated with natural fire. For shrubs, flaming and smoldering combustion were run as separate tests [38], each on a fresh, pre-weighed sample whose $PM_{2.5}$ was collected on its own pre-weighed filter. Samples were placed on a wire-mesh combustion bed and heated with an alcohol lamp; in flaming tests the vapors released during heating were ignited, whereas in smoldering tests the sample was heated without igniting the vapors, so that it burned by flameless oxidation [29]. Both test types burned almost completely (mean residual mass 1.4% and 2.6% of the initial mass). At 40% moisture content flaming could not be sustained, and only smoldering tests were made. After each shrub test the residual mass was recorded.

All experiments used the same standardized ignition procedure to increase replicability of the results. In each experiment, total burn time and peak $PM_{2.5}$ concentration were measured, and remaining mass was recorded for shrubs, with cleaning performed between experiments to avoid contamination. The final dataset contains all 6966 measurements of the design.

2.5. $PM_{2.5}$ Measurement

$PM_{2.5}$ emissions were determined using two complementary devices: gravimetric measurements provided the quantitative figures used in statistical calculations, while optical measurements captured real-time changes in $PM_{2.5}$ concentration during combustion.

2.5.1. Gravimetric Sampling

An environmental mid-flow particulate sampler (model JCH-6120; Qingdao Juchuang Company, Shandong, China) determined $PM_{2.5}$ via a pre-weighed filter membrane. At a constant flow rate of 100 $L \cdot min^{-1}$, a known air volume was drawn through the filter, capturing particles $\leq$ 2.5 μm in aerodynamic diameter. Filters were reconditioned and reweighed post-sampling, and $PM_{2.5}$ mass concentration was calculated from the weight difference divided by sampled air volume.

2.5.2. Continuous Monitoring

The GQ-058 $PM_{2.5}$ air quality analyzer (Shenzhen Jishun'an Technology Co., Ltd., Guangdong, China) provided in situ monitoring of concentration at each combustion stage, based on infrared light scattering by particles, whose intensity depends on particle volume concentration. Mass concentration was then calculated using the device's empirical correlation and calibration. GQ-058 required no sample collection, instead producing continuous concentration traces.

2.5.3. Data Usage

Gravimetric results from JCH-6120 were used for quantification, while real-time results from the GQ-058 instrument were used to investigate the dynamical behavior of $PM_{2.5}$. Because the three vegetation types were initially treated using different experimental procedures, $PM_{2.5}$ is presented in different response forms: mass concentration for broad-leaved trees, and emitted $PM_{2.5}$ mass per combustion test for conifers and shrubs. The research therefore focused on intra-category influencing factors rather than inter-category comparison of $PM_{2.5}$. Only dimensionless quantities (correlation coefficients, ratios, percentage differences, partial η^2 and normalized importances) are therefore compared between categories.

2.5.4. Quality Control

Quality control measures included: (i) instrument calibration against certified $PM_{2.5}$ reference standards at the start of each experimental session, with drift checks at the

end; (ii) pre-test and post-test blank measurements (sampling an empty, ventilated chamber) to quantify background $PM_{2.5}$ levels, which were subtracted from sample readings; (iii) inter-test chamber ventilation and cleaning to prevent carryover contamination; and (iv) replicate consistency checks—the coefficient of variation (CV) across the three replicates of each experimental condition was computed, and any treatment with CV > 50% was flagged for review and repeated when feasible. Triplicate measurements were retained in full for statistical analysis (see below). Outliers were identified using Tukey's 1.5 × IQR rule within each treatment cell, but flagged values were retained in the dataset.

2.6. Emission Factor Calculation

Emission factors were calculated for shrubs, the only category for which residual mass was recorded, as the emitted $PM_{2.5}$ mass per unit initial fuel mass:

$$EF = M\,PM_{2.5}/Mfuel \quad (1)$$

where $M_{PM2.5}$ is the $PM_{2.5}$ mass collected in a test (g) and M_{fuel} is the initial sample mass (g). Combustion was nearly complete (mean residual mass 2.0% of the initial mass), so emission factors based on consumed mass (initial minus residual) differed by less than 3% (mean 12.8 g/kg) and gave the same result for inter-species differences ($p = 0.723$).

2.7. Data Processing and Integration

The naming of the different species used the Latin binomial system using a lookup table. The unified data consisted of species, vegetation category, plant part, season, combustion mode, moisture content, fuel load, wind speed, $PM_{2.5}$ data, and emission factor, forming one coherent dataset consisting of 6966 cases.

2.8. Statistical Analysis

All analyses were performed in R (version 4.6.1) using the tidyverse, car, and multcomp packages. Correlation analysis and linear regression tested the relationship between moisture content and $PM_{2.5}$ emissions within each category, while multi-factor ANOVA assessed main effects and interactions among species, moisture content, fuel load, plant part and the category-specific variable (combustion mode for shrubs, season for broad-leaved species, wind speed for conifers). Main effects were tested with Type II ANOVA (car::Anova) on the main-effects model in Equation (2), and interactions with full-factorial ANOVA. ANOVA assumptions of residual normality and variance homogeneity were tested via Shapiro–Wilk and Levene tests, respectively; where mildly violated, non-parametric methods (Kruskal–Wallis, Wilcoxon rank-sum) supplemented the parametric analysis. Tukey's HSD test identified pairwise differences following significant ANOVA results, and the Wilcoxon rank-sum test compared flaming versus smoldering $PM_{2.5}$ emissions. The multiple linear regression model below

$$PM_{2.5} = \beta_0 + \beta_1 \cdot MC + \beta_2 \cdot FL + \sum \beta_{3i} \cdot Species_i + \sum \beta_{4j} \cdot Part_j + \beta_5 \cdot X + \epsilon \quad (2)$$

was fit for each category, where Part is plant part and X is the category-specific factor (combustion mode for shrubs, wind speed for conifers, season for broad-leaved species). Equation (2) contains the same predictors as the machine-learning models. Model diagnostics included residual plots and variance inflation factors (VIF < 5 for all retained predictors), with all tests conducted at $\alpha = 0.05$. All experiments were run in triplicate per treatment condition, and all triplicates were retained (Section 2.5.4).

2.9. Machine-Learning Modeling

Two ensemble regressors, Random Forest and XGBoost, were used to capture non-linear predictor interactions. Random Forest used the randomForest package with ntree = 500;

mtry was selected per category by grid search over 1–5 minimizing grouped five-fold cross-validated RMSE, giving mtry = 5 for shrubs and mtry = 4 for broad-leaved species and conifers. XGBoost used the xgboost package (η = 0.05, max_depth = 6, nrounds = 300, subsample = 0.8, colsample_bytree = 0.8). Models were fitted separately per vegetation type, reflecting category-specific response variables and predictor sets: species, plant part, moisture content, fuel load, and a category-specific variable (combustion mode for shrubs, season for broad-leaved species, wind speed for conifers). Both models used the same predictors; categorical variables were supplied to Random Forest as factors and to XGBoost as a one-hot design matrix, as required by each implementation. The response variable was the gravimetric $PM_{2.5}$ measurement obtained from the JCH-6120 sampler. For broad-leaved species, $PM_{2.5}$ was expressed as mass concentration ($\mu g\ m^{-3}$), whereas for conifers and shrubs it was expressed as emitted $PM_{2.5}$ mass per combustion test (g). Models were therefore trained and evaluated separately within each vegetation category, and model performance was not interpreted as an absolute comparison across categories. The linear model of Equation (2), evaluated on the same folds, served as the baseline for the ensembles.

Model evaluation used grouped five-fold cross-validation: all replicates of the same treatment condition (the same combination of species, plant part, moisture content, fuel load and the category-specific factor) were assigned to the same fold, so that every out-of-fold prediction was made for a condition not seen during training. RMSE, R^2, and MAE are reported as mean ± SD across folds. Feature importance was computed separately per algorithm: increase in MSE under permutation for Random Forest, total gain for XGBoost. For XGBoost, one-hot encoded features were pooled back into their original names; the importances in each panel were then divided by the largest importance in that panel.

3. Results

3.1. Overall $PM_{2.5}$ Emission Patterns

The 6966 measurements encompassed 2592 conifer, 3240 broad-leaved, and 1134 shrub observations across 22 species (Table S2). All three categories exhibited high variability in $PM_{2.5}$ emissions, with coefficients of variation ranging from 65% (broad-leaved) to 78% (shrub).

Within each category, inter-species variation was present but secondary to the effects of experimental conditions. Among conifers, Picea koraiensis (Korean Spruce) exhibited the highest mean $PM_{2.5}$ (0.032 g), while Picea jezoensis var. microsperma produced the lowest (0.018 g). Among broad-leaved species, Prunus maackii and Acer mono had the highest $PM_{2.5}$ concentrations (~14,800 $\mu g/m^3$), while Prunus padus was lowest (10,905 $\mu g/m^3$). Among shrubs, S. reticulata var. amurensis emitted the most $PM_{2.5}$ (0.026 g) and A. senticosus the least (0.021 g) (Figure S1).

3.2. Primary Controlling Factors by Vegetation Category

3.2.1. Shrubs: Moisture Content, Fuel Load, Plant Part and Combustion Mode

Moisture content was the strongest correlate of $PM_{2.5}$ emissions among shrubs (Pearson r = 0.374, $p < 0.001$, $R^2 = 0.14$), with each percentage-point increase in MC associated with a 7.6×10^{-4} g increase in $PM_{2.5}$ (simple linear regression). In the main-effects ANOVA, moisture content (F = 194.6), fuel load (F = 185.9), plant part (F = 125.4) and combustion mode (F = 14.5) were significant (all $p < 0.001$), whereas species was not (F = 1.86, $p = 0.084$).

Smoldering combustion produced significantly higher $PM_{2.5}$ emissions than flaming (mean 0.026 vs. 0.019 g; Wilcoxon W = 140,225, $p < 0.001$)—a 34% increase (Figure 2)—consistent across all seven species, with S. reticulata var. amurensis showing the largest difference between modes (65%) and A. senticosus the smallest (6%). A significant fuel load × combustion mode interaction (F = 13.1, $p < 0.001$) indicated that the smoldering–flaming difference widened at higher fuel loads.

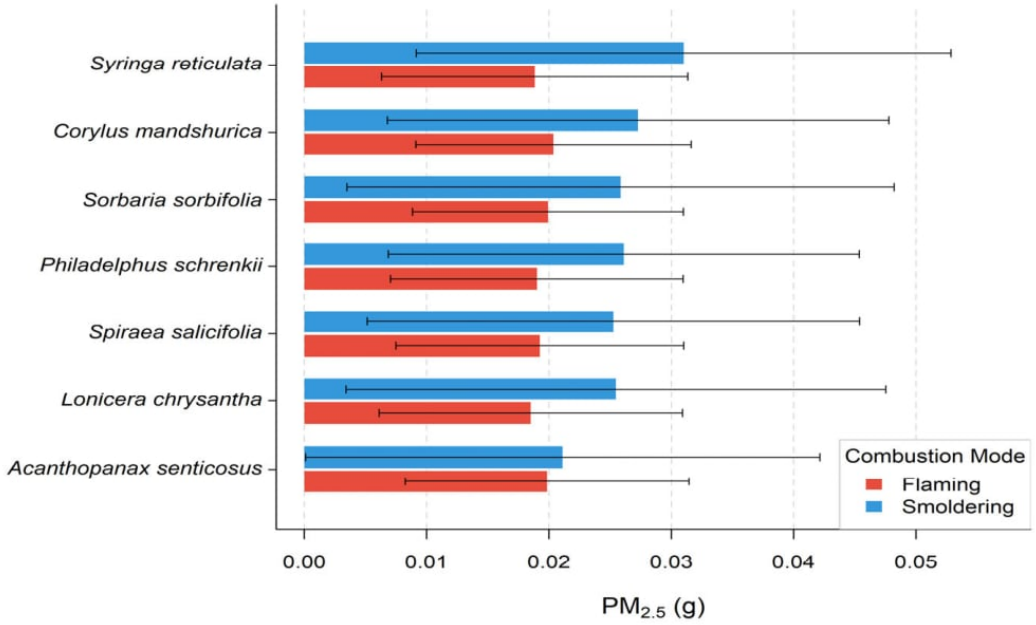

Figure 2. $PM_{2.5}$ emitted in flaming and smoldering tests for seven shrub species. Bars show means and error bars SD over all tests of each species and combustion mode (n = 72 flaming, 90 smoldering), pooling moisture content, fuel load and plant part.

Plant part also had a strong effect. Leaves produced 53% more $PM_{2.5}$ than branches (0.0279 ± 0.0195 vs. 0.0182 ± 0.0145 g; Wilcoxon W = 105,078, $p < 0.001$), and leaves exceeded branches in all seven species (ratio 1.2–2.8). The difference depended on combustion mode: it was large in flaming tests (0.0279 vs. 0.0109 g) but small in smoldering tests (0.0279 vs. 0.0241 g). Branches therefore burned more cleanly when flaming, whereas leaves emitted similar amounts in both modes.

3.2.2. Broad-Leaved Species: Fuel Load, Plant Part, Season and Species

Fuel load was the strongest predictor of broad-leaved $PM_{2.5}$ concentration (F = 1438), followed by plant part (F = 425.9), season (F = 191.1), moisture content (F = 128.7) and species (F = 26.5; all $p < 0.001$). Leaves produced significantly higher $PM_{2.5}$ concentrations (17,297 $\mu g/m^3$) than bark (12,293 $\mu g/m^3$) and branches (10,520 $\mu g/m^3$; all pairwise comparisons significant, Tukey HSD, $p < 0.001$). Because leaves were not sampled in April, seasons were compared for bark and branches only. Their mean $PM_{2.5}$ concentration was highest in April (14,650 $\mu g/m^3$), followed by October (11,818 $\mu g/m^3$) and July (7752 $\mu g/m^3$), so dormant-stage April samples had 89% higher concentrations than July samples. April exceeded July in eight of the nine species (exception: *Acer ukurunduense*). Leaves, sampled in July and October only, had higher concentrations in July (18,822 $\mu g/m^3$) than in October (15,772 $\mu g/m^3$). Significant species × part (F = 15.6, $p < 0.001$) and species × MC (F = 3.8, $p < 0.001$) interactions were also detected, and moisture content showed a weak positive correlation with $PM_{2.5}$ (r = 0.147, $p < 0.001$; Figure S2).

3.2.3. Conifers: Fuel Load, Plant Part and Wind Speed

Among conifers, fuel load, plant part and wind speed were the dominant drivers. Mean $PM_{2.5}$ increased from 0.015 g at 0 m/s to 0.030 g at 1 m/s (a two-fold increase), plateauing at 2–3 m/s (wind speed–$PM_{2.5}$ correlation: r = 0.262, $p < 0.001$), while plant part also significantly affected $PM_{2.5}$: leaves produced the highest emissions (mean 0.036 g), followed by branches (0.025 g) and bark (0.020 g). Unlike shrubs, moisture content showed only a very weak, marginally significant negative correlation with conifer $PM_{2.5}$ emissions

($r = -0.039$, $p = 0.045$, $R^2 = 0.002$); although statistically significant, this association was negligible in magnitude, indicating a negligible role under the tested conditions (MC 0–15%). Fuel load, by contrast, was the dominant predictor ($F = 5188$, $p < 0.001$), followed by wind speed ($F = 712$) and plant part ($F = 632$; both $p < 0.001$). Each additional gram of fuel increased emitted $PM_{2.5}$ by about 0.022 g, with species-specific slopes from 0.014 g/g (*Picea jezoensis* var. *microsperma*) to 0.027 g/g (*Picea koraiensis*).

3.3. Moisture Content Effects Across Categories

The relationship between moisture content and $PM_{2.5}$ emissions differed fundamentally among the three vegetation categories (Figure S3, Table S3). This category-specific pattern extended to the interaction between fuel load and moisture content, which likewise varied across shrubs, broad-leaved species, and conifers (Figure S4).

3.4. Emission Factors

Emission factors were calculated for the seven shrub species (Table S4). The overall mean EF was 0.0125 ± 0.0098 g/g (12.5 g/kg). Values ranged from 0.0116 g/g (A. senticosus) to 0.0135 g/g (S. reticulata var. amurensis). One-way ANOVA detected no significant inter-species differences in EF ($F = 0.678$, $p = 0.668$), indicating comparable $PM_{2.5}$ production per unit initial fuel mass across all shrub species (Figure 3).

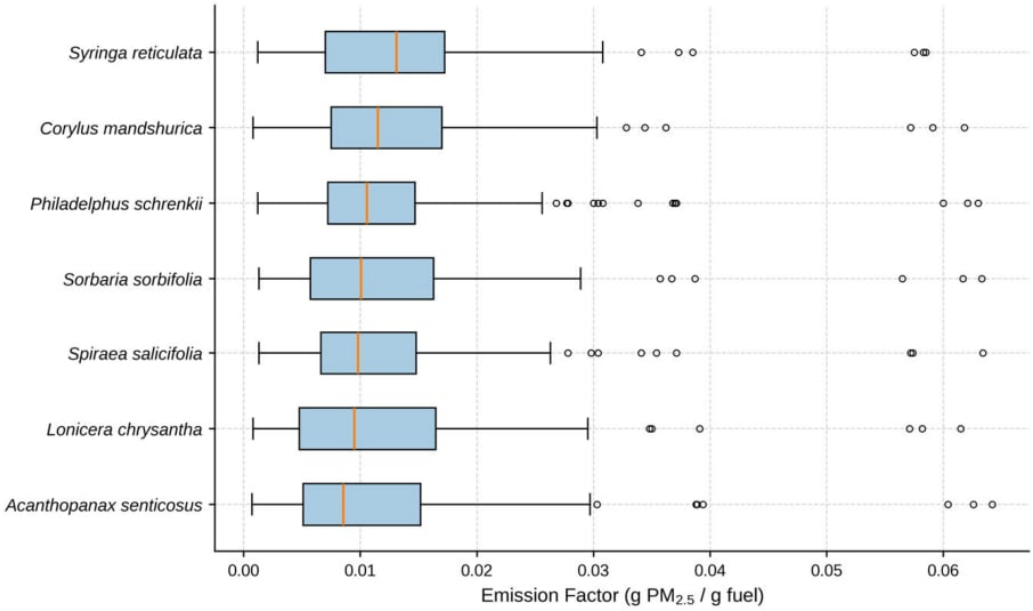

Figure 3. Distribution of $PM_{2.5}$ emission factors across shrub species. No significant inter-species differences ($p = 0.668$). Boxes show the interquartile range (IQR) with the median (orange line); whiskers extend to the most extreme values within 1.5 × IQR; open circles indicate outliers.

3.5. Regression Models

For each vegetation category, multiple linear regression models were constructed, and model summaries are presented in Table S5, with detailed coefficient estimates, standard errors and *p*-values in Table S6. The shrub model had the lowest explanatory power ($R^2 = 0.34$), which is examined below.

The linear models and the machine-learning models used the same predictors in each category.

In the conifer model ($R^2 = 0.75$, $n = 2592$), fuel load, wind speed and plant part were the strongest predictors (all $p < 0.001$), and moisture content had a small negative effect

($p < 0.001$). Leaves emitted 0.016 g and branches 0.005 g more $PM_{2.5}$ than bark. Species identity was also significant ($p < 0.001$): *Picea koraiensis* had the highest emissions and *Picea jezoensis* var. *microsperma* the lowest, both relative to *Abies nephrolepis*; full coefficients appear in Table S6.

The Broad-leaved model ($R^2 = 0.46$, $n = 3240$) was most strongly driven by fuel load, plant part and season, with all p values < 0.001 (Table S6). Leaves yielded significantly higher $PM_{2.5}$ than bark or branches, reflecting their richer volatile content. April samples yielded markedly higher concentrations than July or October collections, in keeping with the higher extractive content of dormant-season fuels. Moisture content had a small positive effect ($p < 0.001$).

The shrub model ($R^2 = 0.34$, $n = 1134$) retained four significant predictors: moisture content, fuel load, plant part and combustion mode (all $p < 0.001$; Table S6). Leaves emitted 0.0097 g and smoldering tests 0.0034 g more $PM_{2.5}$ than branches and flaming tests. Species had no significant overall effect ($p = 0.084$), suggesting that shrub $PM_{2.5}$ is controlled by combustion conditions and tissue type rather than species identity.

The relatively low R^2 (0.34) for the shrub model calls for further investigation. While moisture content, fuel load, plant part, and combustion mode had highly significant main effects, much of the trial-to-trial variability in shrub $PM_{2.5}$ remains unexplained by these covariates, which may partly reflect factors outside the laboratory design: fine-scale heterogeneity in fuel microstructure (e.g., specific leaf area, cuticle thickness, secondary metabolite content) that varies even within a single individual; stochastic combustion dynamics from ignition-front geometry and local chamber turbulence that linear models cannot resolve; and unmeasured chemical traits (lignin-to-cellulose ratio, extractive volatility, ash content) known to affect emission yields independently of bulk moisture or fuel load. However, the non-linear models in Section 3.6 achieved a much higher R^2 under grouped cross-validation (0.87, compared with 0.21 for the linear model), which suggests that the residual variance is mostly attributable to non-linear interactions between these variables, instead of random noise. It is probable that this unexplained variance would be even wider under field conditions due to other uncontrolled factors such as wind, terrain and fuel-bed continuity that are not captured in the laboratory design.

3.6. Machine-Learning Validation

Both ensemble models performed considerably better than linear models with the same predictors evaluated on the same grouped folds (Table S7). Cross-validated R^2 was 0.866 ± 0.049 (Random Forest) and 0.831 ± 0.071 (XGBoost) for shrubs, 0.773 ± 0.042 and 0.867 ± 0.021 for broad-leaved species, and 0.957 ± 0.011 and 0.955 ± 0.006 for conifers, compared with 0.21 ± 0.30, 0.44 ± 0.05 and 0.74 ± 0.03 for the linear models. Random Forest performed best for shrubs and XGBoost for broad-leaved species, and the two were equivalent for conifers. Because every out-of-fold prediction was for a treatment condition absent from training, these values measure prediction of new combinations of factor levels within the tested ranges and species. Figure 4 shows predicted against observed values; scatter is largest for broad-leaved species, where species × part × season interactions are strongest.

Feature-importance rankings (Figure 5) agree with the ANOVA results and highlight plant part. Fuel load was the most important feature for broad-leaved species and conifers in both algorithms. For shrubs, plant part ranked first in XGBoost (1.00) and second in Random Forest (0.85), and moisture content was also high in both (0.84 and 0.55); fuel load ranked first in Random Forest (1.00) but third in XGBoost (0.38), and combustion mode followed (0.85 and 0.36). For broad-leaved species, species ranked second in both algorithms (0.93 and 0.93), followed by season (0.82 and 0.82), plant part (0.81 and 0.58) and moisture content (0.63 and 0.63). For conifers, plant part ranked second (0.74 and 0.33), followed by wind speed (0.65 and 0.30) and species (0.62 and 0.26), with moisture content last (0.45 and 0.06). The algorithms agree on the leading features but differ on secondary

ones, because permutation importance measures the loss of accuracy when a variable is randomized, whereas gain measures its contribution to the split criterion. We therefore treat as robust only features ranked highly by both: plant part and moisture content in shrubs; fuel load, species and season in broad-leaved species; and fuel load, plant part and wind speed in conifers. These importances are within-model measures and are not comparable across categories for factors varied in only one category.

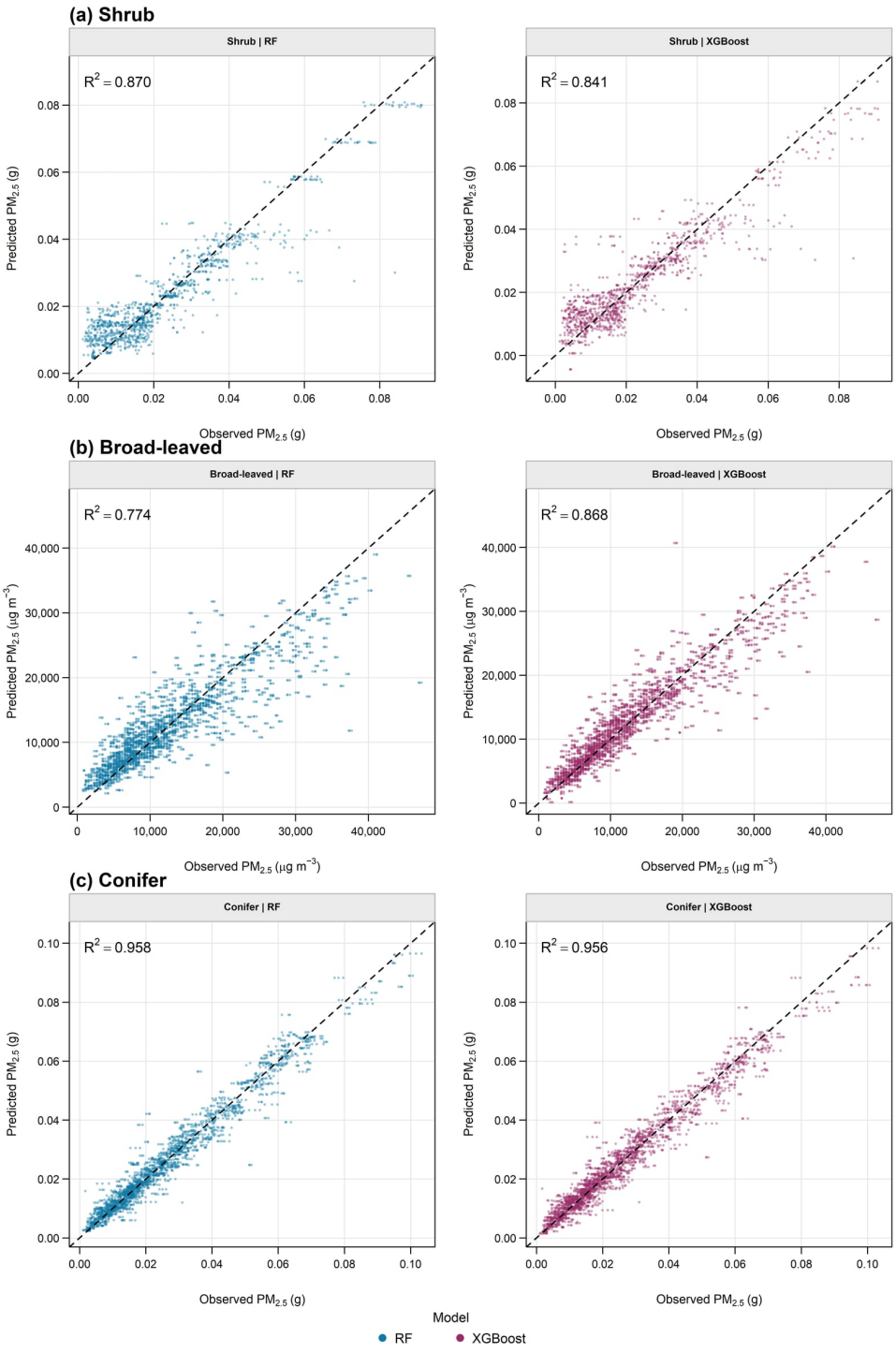

Figure 4. Predicted versus observed $PM_{2.5}$ for Random Forest and XGBoost: (**a**) shrubs (g per test), (**b**) broad-leaved species ($\mu g\ m^{-3}$), (**c**) conifers (g per test). Out-of-fold predictions from grouped five-fold cross-validation (all replicates of a treatment condition in the same fold); dashed line = 1:1; R^2 = pooled out-of-fold R^2.



Figure 5. Normalized feature importance for Random Forest and XGBoost by vegetation category: (**a**) shrubs, (**b**) broad-leaved species, (**c**) conifers. Importances are divided by the largest importance in each panel; permutation importance (%IncMSE) for Random Forest and total gain for XGBoost, with one-hot features pooled to their original variable.

For shrubs, the gain from the linear model ($R^2 = 0.21$ under grouped cross-validation) to Random Forest (0.87) is consistent with the interaction effects identified in Section 3.2.1. Within the tested conditions, this framework provides category-stratified $PM_{2.5}$ predictions; transfer to species outside the training set and to field conditions remains to be tested (Section 4.3).

3.7. Comparison of Shared Factors Across Categories

Because wind speed, season and combustion mode were each varied in only one category, cross-category comparison was restricted to a balanced subset containing only conditions shared by all three categories: July samples, leaves and branches, moisture content 10% and 15%, fuel load 1 g and 2 g, and no forced wind (n = 336 shrub, 216 broad-leaved and 144 conifer measurements). The same main-effects ANOVA was fitted in each category, and effects were compared as partial η^2, which does not depend on the response unit (Table S8). Fuel load had a large effect in all three categories (partial η^2 = 0.24, 0.31 and 0.45 for shrubs, broad-leaved species and conifers). Moisture content had a clear effect only in shrubs (0.16, $p < 0.001$; +55% $PM_{2.5}$ from 10% to 15% moisture), compared with 0.03 in broad-leaved species ($p = 0.014$) and 0.02 in conifers ($p = 0.078$). Species and plant part had large effects in broad-leaved species (0.55 and 0.71) and conifers (0.39 and 0.19) but negligible effects in shrubs (0.02 and 0.00). In shrubs, the plant-part effect was masked by its interaction with combustion mode; within flaming tests alone its partial η^2 was 0.55. Even for the shared factors, therefore, the relative importance of the controls differed among categories.

4. Discussion

The empirical results from the Xiao Xing'an Mountains are incorporated into three integrated core frameworks to describe emission mechanisms, inventory parameters, and operational management constraints.

4.1. Category-Specific Mechanistic and Statistical Emission Drivers

Fuel load was a primary control in all three categories, whereas the secondary controls differed among categories. Because wind speed, season and combustion mode were each varied in only one category, these differences are interpreted within categories, and cross-category comparison is restricted to the shared factors (Section 3.7).

Shrub-Dominated Fuels: Emissions are governed by combustion physics and completeness rather than species identity. The thin, fine-branching architecture yields a high surface-area-to-mass ratio, making efficiency dependent on the thermodynamic competition between moisture evaporation and ignition; elevated moisture prolongs smoldering and suppresses complete oxidation [20,28,57]. The absence of significant inter-species variation within the tested shrub species supports the use of a category-level EF of 12.5 g/kg for similar shrub fuels under comparable combustion conditions, a value highly consistent with global wildland ranges (5–25 g/kg and 7–20 g/kg in North America [22,34], 5.7–14.7 g/kg in southeastern U.S. pine-grasslands [20], biomass burning compilations [27,35], and western North American forest layers [58]).

Broad-Leaved Stands: $PM_{2.5}$ yield is driven primarily by fuel load and secondarily by tissue type. Leaves promote rapid, incomplete combustion due to high volatile content, lower density, and elevated surface-area-to-volume ratios [21,59]. Fuel load exerted the strongest single-factor effect among the broad-leaved factors (F = 1438). Significant species variance (F = 26.5) and species × part interactions (F = 15.6) reflect inter-species divergence in wood density and extractives among the nine broad-leaved genera. In bark and branch fuels, phenological stage produced a clear seasonal pattern (April > October > July); April fuels retain highly flammable winter metabolites (condensed tannins, non-structural carbohydrates, resin-soluble terpenoids) as a chemical defense [60], synchronizing with northeastern China's hazardous spring fire season [45,47].

Conifer Stands: Moisture had a negligible effect on emitted $PM_{2.5}$ mass (r = −0.039), which was contrary to the results seen in shrubs. Resinous and volatile organic matter, which includes monoterpenes and terpenoid extractives found in *Pinus*, *Larix*, and *Picea*, catches fire easily at low temperatures and hence is decoupled from moisture content in

the wood [61]. Wind speed, on the other hand, showed a strong non-linear relationship, as doubling of the mean emitted $PM_{2.5}$ mass was seen when wind speed increased from 0 to 1 m/s, then reached a constant level in the 1–3 m/s range.

Universal Hierarchy: Foliage produced more $PM_{2.5}$ than woody tissues in all three categories: shrub leaves emitted ~1.5 times more than branches, conifer leaves emitted ~1.8 times more $PM_{2.5}$ than bark, and broad-leaved leaves had 1.4-fold higher concentrations than bark (all within-category, dimensionless ratios) [21,59,62]. Volumetric density and volatile content likely explain this pattern, which matches prior Chinese boreal forest data [62].

4.2. Quantitative Inventory Calibration and Cross-Regional Validation

These metrics provide inventory-ready parameters for regional emission modeling, particularly when combined with spatial biomass data, remote-sensing fuel maps, and atmospheric transport models [2,17]. The mean shrub EF (12.5 g/kg) matches independent estimates from North American biomes [20,22,34], rural Chinese biomass (2.5–17.8 g/kg) [59], and the Daxing'an Mountains [48]. Because shrub EF shows no significant inter-species variance, it can be applied as a single scaling value—unlike the broad-leaved category, where species identity must be resolved explicitly ($p < 0.001$).

Beyond static EFs, the regression coefficients yield direct landscape conversion parameters. Conifer fuel load converts to $PM_{2.5}$ at a near-linear rate of ~2.2% ($\beta = 0.022$ g/g) [22,35]. Broad-leaved concentrations, by contrast, are dominated by fuel mass ($\beta = 5030$ μg/m^3 per gram) and tissue type ($\beta = 6625$ μg/m^3, leaf vs. bark). This study's shrub EF (≈12.5 g/kg) falls below highly smoldering tropical or boreal peat systems (≥30 g/kg) [63] but slightly exceeds open airborne plume values—consistent with near-source capture before atmospheric dilution.

4.3. Fire Management, Climate Projections, and Methodological Scope

The factor-level interactions identified above carry direct implications for forestry practice, with distinct trade-offs and limits for each vegetation category:

Smoke-Aware Management Applications: Shrub fuel beds need precise moisture thresholds so that prescribed burns can be scheduled under clean-flaming conditions (low moisture), minimizing fine-particle emissions [1]. In broad-leaved stands, bark and branch fuels emitted least in July, whereas leaves emitted most in July, so the timing of fuel reduction should depend on which fuel component dominates the treated fuel bed. Conifer ignition planning should account for the 0–1 m/s threshold at which emissions double [34,56]. Unlike uniform national pre-suppression and seasonal fire-ban policies [1,56], these adjustments are specific to each vegetation category.

Climate warming and intensifying spring droughts in northeastern China are projected to continue [64,65]. Under these conditions, shrub encroachment into post-fire disturbances could shift regional emissions toward the more moisture-sensitive shrub regime, raising the public-health smoke burden. Changes in wind conditions during dry periods may modify conifer $PM_{2.5}$ emissions, although this interaction requires field-scale validation.

Methodological Limitations: Six experimental parameters constrain the usefulness of the current framework:

- Unbalanced Cross-Category Design: Wind speed, season and combustion mode were each varied in only one category (Table 1). Their effects cannot be compared across categories, and part of the apparent category specificity reflects the design rather than fuel behavior. Only species, plant part, moisture content and fuel load can be compared across categories (Section 3.7); a design with all factors crossed in all categories is needed to test category specificity directly.

- Model Transferability: Grouped cross-validation tests new combinations of factor levels for the species studied. The models were not tested on species outside the training set or on field burns.
- Chamber Scale: Lab-scale setups examine each factor parameter individually, increasing internal validity, while landscape-scale output brings structural bed parameters into the equation [66].
- Response Format Variance: Broad-leaved measurements are based on filter concentrations ($\mu g/m^3$) while conifers and shrubs are measured in absolute mass (g), reflecting the different sampling protocols required for each fuel type. Shrub emission factors are expressed on a mass basis (g $PM_{2.5}$ per g fuel) and are therefore independent of sampled air volume; only the broad-leaved concentrations depend on the sampled volume. Values are therefore not comparable in absolute magnitude across vegetation categories, and all analyses were conducted within each category separately.
- Chemical Speciation Gaps: Current measures capture gravimetric mass changes. Future chemical speciation analysis (EC/OC, water-soluble ions, trace metals, molecular tracers) would be the next step toward source apportionment [67–69], and can use known ionic signatures [68], trace metal sources [70], and biofuel tracers [71].
- Wind Velocity Constraints: The 3 m/s limit captures laminar in-stand air flow but not turbulent fire-atmosphere interaction (5–10 m/s). Interpret all reported conifer wind response results as a conservative lower bound.

5. Conclusions

This study examined $PM_{2.5}$ emissions from 22 forest fuel species in three vegetation categories of the Xiao Xing'an Mountains. Fuel load was a primary factor in all three categories. In addition, $PM_{2.5}$ was controlled by moisture content, plant part and combustion mode in shrubs; by plant part, season and species in broad-leaved species; and by plant part and wind speed in conifers. Because wind speed, season and combustion mode were each tested in only one category, these results describe within-category behavior; among the shared factors, moisture content had a clear effect only in shrubs, whereas, in the balanced subset, species and plant part mattered in trees but not in shrubs. Smoldering tests produced 34% more $PM_{2.5}$ than flaming tests in shrubs ($p < 0.001$), and leaves emitted more than other plant parts in all three categories. Shrub emission factors averaged 12.5 g/kg with no significant difference among species ($p = 0.668$), supporting a single value for parameterization. Broad-leaved bark and branches had 89% higher $PM_{2.5}$ concentrations in April than in July, consistent with the regional spring fire season.

This research thus provides a shrub $PM_{2.5}$ emission factor and category-specific emission parameters for the Xiao Xing'an Mountains, supports including vegetation category as a stratification variable in forest-fire emission inventories, and supports development of a local emission model for mixed coniferous-broad-leaved forests in northeast China.

Three natural extensions of this work are identified: (1) size-resolved measurements distinguishing $PM_{2.5}$ from PM_{10} and coarser fractions to connect these findings to health-impact metrics; (2) chemical speciation of the emitted aerosol to support source apportionment and atmospheric chemistry applications; and (3) integration of the derived emission factors with remote-sensing-based fuel load maps to generate regional-scale $PM_{2.5}$ emission inventories for the Xiao Xing'an Mountains and comparable temperate forest ecosystems. Field-scale validation under instrumented prescribed burns remains the natural next test before applying these category-specific coefficients to predictive emission modeling.

Under grouped five-fold cross-validation, Random Forest and XGBoost models trained separately for each category reached R^2 of 0.77–0.96, compared with 0.21–0.74 for linear models with the same predictors; Random Forest performed best for shrubs, XGBoost for broad-leaved species, and the two were equivalent for conifers. Feature-importance rankings were consistent with the main controls identified by ANOVA and provide a reproducible baseline for regional emission-inventory frameworks within the tested conditions.

Supplementary Materials: The following supporting information can be downloaded at: https://www.mdpi.com/article/10.3390/fire9110493/s1, Table S1: Species included in combustion experiments; Table S2: Summary of $PM_{2.5}$ emissions by vegetation category; Table S3: Correlation between moisture content and $PM_{2.5}$ emissions; Table S4: $PM_{2.5}$ emission factors for shrub species (mean ± SD); Table S5: Summary of multiple regression models for $PM_{2.5}$ prediction; Table S6: Key regression coefficients for category-specific $PM_{2.5}$ prediction models; Table S7: Grouped five-fold cross-validated performance of machine-learning and linear models for $PM_{2.5}$ prediction (mean ± SD across folds); Table S8: Partial η^2 of shared factors in the balanced common subset (Type II ANOVA); Figure S1: Mean $PM_{2.5}$ emissions (± SD) by species for (a) shrubs, (b) broad-leaved species, and (c) conifers; Figure S2: Mean $PM_{2.5}$ concentration ($\mu g/m^3$) for broad-leaved species by moisture content; Figure S3: $PM_{2.5}$ emissions as a function of moisture content for (a) shrubs, (b) broad-leaved species, and (c) conifers; Figure S4: Interaction between fuel load and moisture content on $PM_{2.5}$ emissions for (a) shrubs, (b) broad-leaved species, and (c) conifers.

Author Contributions: D.A.: Conceptualization, Methodology, Software, Investigation, Data curation, Visualization, Writing—original draft, Writing—review & editing. H.H.: Validation, Supervision. H.G.: Supervision. X.H.: Supervision. M.A.: Formal analysis. S.A.: Writing—review & editing. X.Z.: Supervision. Z.S.: Conceptualization, Validation, Resources, Data curation, Funding acquisition, Supervision, Project administration. All authors have read and agreed to the published version of the manuscript.

Funding: This research was funded by the Undergraduate Education and Teaching Research Project at Northeast Forestry University (grant no. DGY2025-06), Heilongjiang Provincial Natural Science Foundation Joint Fund Support Project (grant no. PL2026C146), and the National Key R&D Program of China (grant no. 2024YFF1306200, 2024YFF1306203). The funders had no role in the design of the study; in the collection, analysis, or interpretation of data; in the writing of the manuscript; or in the decision to publish the results.

Institutional Review Board Statement: Not applicable.

Informed Consent Statement: Not applicable.

Data Availability Statement: The data supporting this study are openly available in Mendeley Data at https://doi.org/10.17632/hjp3gy72cp.3.

Acknowledgments: The authors thank Northeast Forestry University for providing laboratory facilities and combustion chamber access, and the local forestry bureaus and the Liangshui National Nature Reserve for their assistance with fuel sample collection. Icons used in the graphical abstract were designed by Freepik, www.freepik.com (accessed on 2 November 2026); additional icons were sourced from SVG Repo (CC0), www.svgrepo.com (accessed on 2 November 2026).

Conflicts of Interest: The authors declare no conflicts of interest.

Abbreviations

The following abbreviations are used in this manuscript:

$PM_{2.5}$	Fine particulate matter (aerodynamic diameter ≤ 2.5 μm)
MC	Moisture Content
FL	Fuel Load
EF	Emission Factor
ANOVA	Analysis of Variance

CV	Coefficient of Variation
SD	Standard Deviation
VIF	Variance Inflation Factor
IQR	Interquartile Range
HSD	Honestly Significant Difference
RMSE	Root Mean Square Error
MAE	Mean Absolute Error
IPCC	Intergovernmental Panel on Climate Change

References

1. Jaffe, D.A.; O'Neill, S.M.; Larkin, N.K.; Holder, A.L.; Peterson, D.L.; Halofsky, J.E.; Rappold, A.G. Wildfire and Prescribed Burning Impacts on Air Quality in the United States. *J. Air Waste Manag. Assoc.* **2020**, *70*, 583–615. [CrossRef] [PubMed]
2. Song, R.; Wang, T.; Han, J.; Xu, B.; Ma, D.; Zhang, M.; Li, S.; Zhuang, B.; Li, M.; Xie, M. Spatial and Temporal Variation of Air Pollutant Emissions from Forest Fires in China. *Atmos. Environ.* **2022**, *281*, 119156. [CrossRef]
3. Hu, Q.; Wang, Y.; Wang, Y.; He, C. The Dynamic Evolution Characteristics of PM2.5 Concentrations and Health Risk Assessment during Typical Forest Fires in China. *Atmos. Pollut. Res.* **2024**, *15*, 102303. [CrossRef]
4. Jin, Z.; Ferrada, G.A.; Zhang, D.; Scovronick, N.; Fu, J.S.; Chen, K.; Liu, Y. Fire Smoke Elevated the Carbonaceous PM2.5 Concentration and Mortality Burden in the Contiguous U.S. and Southern Canada. *Environ. Sci. Technol.* **2025**, *59*, 12196–12210. [CrossRef] [PubMed]
5. Scarpa, C.; Bacciu, V.; Ascoli, D.; Costa-Saura, J.M.; Salis, M.; Sirca, C.; Marchetti, M.; Spano, D. Estimating Annual GHG and Particulate Matter Emissions from Rural and Forest Fires Based on an Integrated Modelling Approach. *Sci. Total Environ.* **2024**, *907*, 167960. [CrossRef] [PubMed]
6. Yabo, S.D.; Fu, D.; Li, B.; Ma, L.; Shi, X.; Lu, L.; Shengjin, X.; Meng, F.; Jiang, J.; Zhang, W.; et al. Synergistic Interactions of Fine Particles and Radiative Effects in Modulating Urban Heat Islands during Winter Haze Event in a Cold Megacity of Northeast China. *Environ. Sci. Pollut. Res.* **2023**, *30*, 58882–58906. [CrossRef] [PubMed]
7. Liu, J.C.; Mickley, L.J.; Sulprizio, M.P.; Dominici, F.; Yue, X.; Ebisu, K.; Anderson, G.B.; Khan, R.F.A.; Bravo, M.A.; Bell, M.L. Particulate Air Pollution from Wildfires in the Western US under Climate Change. *Clim. Change* **2016**, *138*, 655–666. [CrossRef] [PubMed]
8. Van Der Werf, G.R.; Randerson, J.T.; Giglio, L.; Van Leeuwen, T.T.; Chen, Y.; Rogers, B.M.; Mu, M.; Van Marle, M.J.E.; Morton, D.C.; Collatz, G.J.; et al. Global Fire Emissions Estimates during 1997–2016. *Earth Syst. Sci. Data* **2017**, *9*, 697–720. [CrossRef]
9. IPCC. *Climate Change 2021: The Physical Science Basis*; IPCC: Geneva, Switzerland, 2021.
10. Jin, Q.; Wang, W.; Zheng, W.; Innes, J.L.; Wang, G.; Guo, F. Dynamics of Pollutant Emissions from Wildfires in Mainland China. *J. Environ. Manag.* **2022**, *318*, 115499. [CrossRef] [PubMed]
11. Zhao, F.; Liu, Y.; Shu, L.; Zhang, Q. Wildfire Smoke Transport and Air Quality Impacts in Different Regions of China. *Atmosphere* **2020**, *11*, 941. [CrossRef]
12. Li, C.; Liu, M.; Hu, Y.; Zhou, R.; Huang, N.; Wu, W.; Liu, C. Spatial Distribution Characteristics of Gaseous Pollutants and Particulate Matter inside a City in the Heating Season of Northeast China. *Sustain. Cities Soc.* **2020**, *61*, 102302. [CrossRef]
13. Zhang, J.; Liu, L.; Xu, L.; Lin, Q.; Zhao, H.; Wang, Z.; Guo, S.; Hu, M.; Liu, D.; Shi, Z.; et al. Exploring Wintertime Regional Haze in Northeast China: Role of Coal and Biomass Burning. *Atmos. Chem. Phys.* **2020**, *20*, 5355–5372. [CrossRef]
14. Zhang, L.; Liu, Y.; Hao, L. Contributions of Open Crop Straw Burning Emissions to $PM_{2.5}$ Concentrations in China. *Environ. Res. Lett.* **2016**, *11*, 014014. [CrossRef]
15. Zhao, H.; Yang, G.; Xiu, A.; Zhang, X. A High Resolution Emission Inventory of Domestic Burning in Rural Region of Northeast China Based on Household Consumption. *Chin. Geogr. Sci.* **2020**, *30*, 921–933. [CrossRef]
16. Wang, S.; Feng, H.; Zou, B.; Yang, Z.; Ding, Y. Correlation between Biomass Burning and Air Pollution in China: Spatial Heterogeneity and Corresponding Factors. *Glob. Planet. Change* **2022**, *213*, 103823. [CrossRef]
17. Li, B.; Xu, Z.; Liu, B.; Zhang, Z.; Qiu, W.; Wang, W. Development of a Finer-Resolution Multi-Year Emission Inventory for Open Biomass Burning in Heilongjiang Province, China. *Sci. Rep.* **2024**, *14*, 29969. [CrossRef] [PubMed]
18. Chen, L.; Gao, Y.; Ma, M.; Wang, L.; Wang, Q.; Guan, S.; Yao, X.; Gao, H. Striking Impacts of Biomass Burning on PM2.5 Concentrations in Northeast China through the Emission Inventory Improvement. *Environ. Pollut.* **2023**, *318*, 120835. [CrossRef] [PubMed]
19. Aleksandrov, A.A.; Ksenofontov, B.S.; Kozodaev, A.S.; Taranov, R.A.; Vyazova, V.D.; Ivanov, M.V. Development of an Algorithm for Calculating the Moisture Content and Time of Forest Fire Maturation of Forest Combustible Materials for Determining Forest Fire Hazards. *Electronics* **2023**, *12*, 1937. [CrossRef]
20. Robertson, K.M.; Hsieh, Y.P.; Bugna, G.C. Fire Environment Effects on Particulate Matter Emission Factors in Southeastern U.S. Pine-Grasslands. *Atmos. Environ.* **2014**, *99*, 104–111. [CrossRef]

21. Dong, T.T.T.; Stock, W.D.; Callan, A.C.; Strandberg, B.; Hinwood, A.L. Emission Factors and Composition of PM2.5 from Laboratory Combustion of Five Western Australian Vegetation Types. *Sci. Total Environ.* **2020**, *703*, 134796. [CrossRef] [PubMed]
22. Hosseini, S.; Urbanski, S.P.; Dixit, P.; Qi, L.; Burling, I.R.; Yokelson, R.J.; Johnson, T.J.; Shrivastava, M.; Jung, H.S.; Weise, D.R.; et al. Laboratory Characterization of PM Emissions from Combustion of Wildland Biomass Fuels. *J. Geophys. Res. Atmos.* **2013**, *118*, 9914–9929. [CrossRef]
23. Zhang, Y.; Obrist, D.; Zielinska, B.; Gertler, A. Particulate Emissions from Different Types of Biomass Burning. *Atmos. Environ.* **2013**, *72*, 27–35. [CrossRef]
24. Zheng, H.; Peng, X.; Zhang, M.; Hu, D.; Xia, Z. Characteristics of Carbon-Containing Gases Release During Combustion of Main Arbor in Heilongjiang Province of China. *Procedia Eng.* **2013**, *52*, 645–651. [CrossRef]
25. Williams, A.; Jones, J.M.; Ma, L.; Pourkashanian, M. Pollutants from the Combustion of Solid Biomass Fuels. *Prog. Energy Combust. Sci.* **2012**, *38*, 113–137. [CrossRef]
26. Yang, H.; Yan, R.; Chen, H.; Lee, D.H.; Zheng, C. Characteristics of Hemicellulose, Cellulose and Lignin Pyrolysis. *Fuel* **2007**, *86*, 1781–1788. [CrossRef]
27. Andreae, M.O. Emission of Trace Gases and Aerosols from Biomass Burning—An Updated Assessment. *Atmos. Chem. Phys.* **2019**, *19*, 8523–8546. [CrossRef]
28. Chen, P.; Li, Y.; Zhang, Y.; Xue, C.; Hopke, P.K.; Li, X. Dynamic Changes of Composition of Particulate Matter Emissions during Residential Biomass Combustion. *Environ. Sci. Technol.* **2023**, *57*, 15193–15202. [CrossRef] [PubMed]
29. Tang, S.; Yin, S.; Shan, Y.; Yu, B.; Cui, C.; Cao, L. The Characteristics of Gas and Particulate Emissions from Smouldering Combustion in the Pinus Pumila Forest of Huzhong National Nature Reserve of the Daxing'an Mountains. *Forests* **2023**, *14*, 364. [CrossRef]
30. Christian, T.J.; Kleiss, B.; Yokelson, R.J.; Holzinger, R.; Crutzen, P.J.; Hao, W.M.; Saharjo, B.H.; Ward, D.E. Comprehensive Laboratory Measurements of Biomass-burning Emissions: 1. Emissions from Indonesian, African, and Other Fuels. *J. Geophys. Res. Atmos.* **2003**, *108*, 2003JD003704. [CrossRef]
31. McMeeking, G.R.; Kreidenweis, S.M.; Baker, S.; Carrico, C.M.; Chow, J.C.; Collett, J.L.; Hao, W.M.; Holden, A.S.; Kirchstetter, T.W.; Malm, W.C.; et al. Emissions of Trace Gases and Aerosols during the Open Combustion of Biomass in the Laboratory. *J. Geophys. Res. Atmos.* **2009**, *114*, 2009JD011836. [CrossRef]
32. Stockwell, C.E.; Yokelson, R.J.; Kreidenweis, S.M.; Robinson, A.L.; DeMott, P.J.; Sullivan, R.C.; Reardon, J.; Ryan, K.C.; Griffith, D.W.T.; Stevens, L. Trace Gas Emissions from Combustion of Peat, Crop Residue, Domestic Biofuels, Grasses, and Other Fuels: Configuration and Fourier Transform Infrared (FTIR) Component of the Fourth Fire Lab at Missoula Experiment (FLAME-4). *Atmos. Chem. Phys.* **2014**, *14*, 9727–9754. [CrossRef]
33. Selimovic, V.; Yokelson, R.J.; Warneke, C.; Roberts, J.M.; De Gouw, J.; Reardon, J.; Griffith, D.W.T. Aerosol Optical Properties and Trace Gas Emissions by PAX and OP-FTIR for Laboratory-Simulated Western US Wildfires during FIREX. *Atmos. Chem. Phys.* **2018**, *18*, 2929–2948. [CrossRef]
34. Prichard, S.J.; O'Neill, S.M.; Eagle, P.; Andreu, A.G.; Drye, B.; Dubowy, J.; Urbanski, S.; Strand, T.M. Wildland Fire Emission Factors in North America: Synthesis of Existing Data, Measurement Needs and Management Applications. *Int. J. Wildland Fire* **2020**, *29*, 132–147. [CrossRef]
35. Akagi, S.K.; Yokelson, R.J.; Wiedinmyer, C.; Alvarado, M.J.; Reid, J.S.; Karl, T.; Crounse, J.D.; Wennberg, P.O. Emission Factors for Open and Domestic Biomass Burning for Use in Atmospheric Models. *Atmos. Chem. Phys.* **2011**, *11*, 4039–4072. [CrossRef]
36. Lu, B.; Huang, H.; Wu, Z.; Zhang, T.; Gu, Y.; Wang, F.; Shu, Z. Utilizing LightGBM to Explore the Characterization of PM2.5 Emission Patterns from Broadleaf Tree Combustion in Northeastern China. *Forests* **2025**, *16*, 836. [CrossRef]
37. Gu, Y.; Han, X.; Gao, H.; Wu, Z.; Zhang, T.; Lu, B.; Shu, Z. Investigating the Characteristics of PM2.5 Emissions from Coniferous Trees during Indoor Simulated Combustion Utilizing a Random Forest Model. *Front. For. Glob. Change* **2026**, *9*, 1744104. [CrossRef]
38. Zhang, T.; Han, X.; Gao, H.; Huang, H.; Wu, Z.; Gu, Y.; Lu, B.; Shu, Z. Development of a PM2.5 Emission Factor Prediction Model for Shrubs in the Xiao Xing'an Mountains Based on Coupling Effects of Physical Factors. *Forests* **2026**, *17*, 199. [CrossRef]
39. Liu, D.; Zhang, N.C.; Liu, G.J. Investigation and Analysis of the Relationship Between Forest Fuels and Stand Characteristics in Lesser Khingan Mountains. *For. Fire Prev.* **2023**, *41*, 21–25.
40. Zhang, N.N.; Liu, Z.G. Trade-Offs/Synergies of Ecosystem Services in the Xiaoxing'an Mountains Based on the InVEST Model. *Environ. Sci.* **2025**, *46*, 4628–4640. [CrossRef] [PubMed]
41. Lv, X.Z.; Jia, W.W. Distribution and Modelling of Carbon Stocks in Understory Vegetation and Young Trees in the Lesser Khingan Mountains Forests. *J. Southwest For. Univ.* **2025**, *45*, 130–138.
42. Wang, H.X.; Cai, T.J.; Jing, J.X.; Yang, C.G.; Yang, H.Y. Carbon Storage and Its Distribution Characteristics of Three Artificial Forests in the Xiaoxing'an Mountains. *For. Investig. Des.* **2025**, *54*, 24–31.
43. Zhang, N.C.; Liu, G.J.; Cui, W.F. Study on the Combustibility of 12 Shrub Species in the Xiao Xing'an Mountains. *For. Eng.* **2025**, *41*, 75–85.

44. Guo, Y.; Cui, S.; Liu, Y.B.; Pan, M.Y.; Sun, G.Z.; Sun, Y.M.; Xiao, R. Additive Biomass Models for Four Main Shrub Species in Xiaoxing'an Mountains. *For. Eng*. **2025**, *42*, 738.
45. Ga, R.; Liu, X.; Ma, B.; Na, M.; Zhang, J.; Tong, Z.; Wei, X.; Xu, J. The Individual and Combined Effects of Natural–Human Factors on Forest Fire Frequency in Northeast China. *Remote Sens*. **2025**, *17*, 1685. [CrossRef]
46. Zhang, B.; Cai, D.; Ai, S.; Wang, H.; Zuo, X. Research on the Influencing Factors and Prevention Measures of Long-Term Forest Fire Risk in Northeast China. *Ecol. Indic*. **2023**, *155*, 110965. [CrossRef]
47. Zhang, Y.; Hu, H.; Wang, Q. Carbon Emissions from Forest Fires in Great Xing'an Mountains from 1980 to 2005. *Procedia Environ. Sci*. **2011**, *10*, 2505–2510. [CrossRef]
48. Zhang, H.; Li, H.; Liu, X.; Ma, Y.; Zhou, Q.; Sa, R.; Zhang, Q. Emissions Released by Forest Fuel in the Daxing'an Mountains, China. *Forests* **2022**, *13*, 1220. [CrossRef]
49. Wu, Z.; Hasham, A.; Zhang, T.; Gu, Y.; Lu, B.; Sun, H.; Shu, Z. Analysis of PM2.5 Concentration Released from Forest Combustion in Liangshui National Natural Reserve, China. *Fire* **2024**, *7*, 311. [CrossRef]
50. Zhang, W.; Yang, Y.; Hu, C.; Zhang, L.; Hou, B.; Wang, W.; Li, Q.; Li, Y. NPP and Carbon Emissions under Forest Fire Disturbance in Southwest and Northeast China from 2001 to 2020. *Forests* **2023**, *14*, 999. [CrossRef]
51. Wang, B.; Mu, C.; Lu, H.; Li, N.; Zhang, Y.; Ma, L. Ecosystem Carbon Storage and Sink/Source of Temperate Forested Wetlands in Xiaoxing'anling, Northeast China. *J. For. Res*. **2022**, *33*, 839–849. [CrossRef]
52. Yang, J.; Huang, X. The 30 m Annual Land Cover Dataset and Its Dynamics in China from 1990 to 2019. *Earth Syst. Sci. Data* **2021**, *13*, 3907–3925. [CrossRef]
53. Hu, J.T.; Liu, J.G.; Wang, C.K.; Zhang, Q.Z. The Difference in Forest Carbon Density and Its Influencing Factors at Different Latitudes in the Xiaoxing'an Mountains. *Acta Ecol. Sin*. **2025**, *45*, 11763–11776.
54. Shan, W.; Xu, Z.; Guo, Y.; Zhang, C.; Hu, Z.; Wang, Y. Geological Methane Emissions and Wildfire Risk in the Degraded Permafrost Area of the Xiao Xing'an Mountains, China. *Sci. Rep*. **2020**, *10*, 21297. [CrossRef] [PubMed]
55. Sun, P.; Qu, Z.; Yuan, C.; Yuan, Y.; Wang, C.; Jia, Q. Meteorological Tower Observed CO2 Flux and Footprint in the Forest of Xiaoxing'an Mountains, Northeast China. *J. Meteorol. Res*. **2023**, *37*, 126–140. [CrossRef]
56. He, H.; Chang, Y.; Liu, Z.H.; Xiong, Z.P.; Bu, R.C. Effects of Fuel Treatments on Forest Fire Regimes under Different Fire Control Policies in the Great Xing'an. *Chin. J. Ecol*. **2024**, *43*, 305–313.
57. Ma, Y.; Zheng, W.; Guo, X.; Tigabu, M.; Guo, F. Effect of Forest Floor Fuel Moisture Content on Chemical Components of PM2.5 Emitted during Combustion. *Chemosphere* **2021**, *279*, 130547. [CrossRef] [PubMed]
58. Urbanski, S.P.; Long, R.W.; Halliday, H.; Lincoln, E.N.; Habel, A.; Landis, M.S. Fuel Layer Specific Pollutant Emission Factors for Fire Prone Forest Ecosystems of the Western U.S. and Canada. *Atmos. Environ. X* **2022**, *16*, 100188. [CrossRef] [PubMed]
59. Shen, G.; Wei, S.; Wei, W.; Zhang, Y.; Min, Y.; Wang, B.; Wang, R.; Li, W.; Shen, H.; Huang, Y.; et al. Emission Factors, Size Distributions, and Emission Inventories of Carbonaceous Particulate Matter from Residential Wood Combustion in Rural China. *Environ. Sci. Technol*. **2012**, *46*, 4207–4214. [CrossRef] [PubMed]
60. Bryant, J.P.; Chapin, F.S.; Klein, D.R. Carbon/Nutrient Balance of Boreal Plants in Relation to Vertebrate Herbivory. *Oikos* **1983**, *40*, 357. [CrossRef]
61. Geron, C.; Rasmussen, R.; Arnts, R.R.; Guenther, A. A Review and Synthesis of Monoterpene Speciation from Forests in the United States. *Atmos. Environ*. **2000**, *34*, 1761–1781. [CrossRef]
62. Guo, L.; Ma, Y.; Tigabu, M.; Guo, X.; Zheng, W.; Guo, F. Emission of Atmospheric Pollutants during Forest Fire in Boreal Region of China. *Environ. Pollut*. **2020**, *264*, 114709. [CrossRef] [PubMed]
63. Stockwell, C.E.; Jayarathne, T.; Cochrane, M.A.; Ryan, K.C.; Putra, E.I.; Saharjo, B.H.; Nurhayati, A.D.; Albar, I.; Blake, D.R.; Simpson, I.J.; et al. Field Measurements of Trace Gases and Aerosols Emitted by Peat Fires inCentral Kalimantan, Indonesia, during the 2015 El Niño. *Atmos. Chem. Phys*. **2016**, *16*, 11711–11732. [CrossRef]
64. Liu, Z.; Yang, J.; Chang, Y.; Weisberg, P.J.; He, H.S. Spatial Patterns and Drivers of Fire Occurrence and Its Future Trend under Climate Change in a Boreal Forest of Northeast China. *Glob. Change Biol*. **2012**, *18*, 2041–2056. [CrossRef]
65. Mack, M.C.; Bret-Harte, M.S.; Hollingsworth, T.N.; Jandt, R.R.; Schuur, E.A.G.; Shaver, G.R.; Verbyla, D.L. Carbon Loss from an Unprecedented Arctic Tundra Wildfire. *Nature* **2011**, *475*, 489–492. [CrossRef] [PubMed]
66. Yokelson, R.J.; Burling, I.R.; Gilman, J.B.; Warneke, C.; Stockwell, C.E.; De Gouw, J.; Akagi, S.K.; Urbanski, S.P.; Veres, P.; Roberts, J.M.; et al. Coupling Field and Laboratory Measurements to Estimate the Emission Factors of Identified and Unidentified Trace Gases for Prescribed Fires. *Atmos. Chem. Phys*. **2013**, *13*, 89–116. [CrossRef]
67. Li, M.; Xu, Z.; Dong, Z.; Deng, J.; Fu, P.; Pavuluri, C.M. Chemical and Stable Carbon Isotopic Compositions of $PM_{2.5}$ from Two Typical Forests in China: Implication for Sources. *Biogeosciences* **2025**, *22*, 5329–5347. [CrossRef]
68. Ma, Y.; Tigabu, M.; Guo, X.; Zheng, W.; Guo, L.; Guo, F. Water-Soluble Inorganic Ions in Fine Particulate Emission During Forest Fires in Chinese Boreal and Subtropical Forests: An Indoor Experiment. *Forests* **2019**, *10*, 994. [CrossRef]

69. Permar, W.; Wang, Q.; Selimovic, V.; Wielgasz, C.; Yokelson, R.J.; Hornbrook, R.S.; Hills, A.J.; Apel, E.C.; Ku, I.; Zhou, Y.; et al. Emissions of Trace Organic Gases From Western U.S. Wildfires Based on WE-CAN Aircraft Measurements. *J. Geophys. Res. Atmos.* **2021**, *126*, e2020JD033838. [CrossRef]
70. Li, C.; Bai, L.; Qin, J.; Guo, Y.; Wang, H.; Xu, X. Study on Metal Elements in Indoor Particulate Matter: A Case Study of Rural Residential Environment in Northeast China. *Environ. Geochem. Health* **2023**, *45*, 4867–4881. [CrossRef] [PubMed]
71. Tao, J.; Zhang, Z.; Zhang, L.; Huang, D.; Wu, Y. Quantifying the Relative Importance of Major Tracers for Fine Particles Released from Biofuel Combustion in Households in the Rural North China Plain. *Environ. Pollut.* **2021**, *268*, 115764. [CrossRef] [PubMed]

Disclaimer/Publisher's Note: The statements, opinions and data contained in all publications are solely those of the individual author(s) and contributor(s) and not of MDPI and/or the editor(s). MDPI and/or the editor(s) disclaim responsibility for any injury to people or property resulting from any ideas, methods, instructions or products referred to in the content.